98-003

Paper No.
294

CORROSION 98

THE ROLE OF BIOMINERALIZATION IN MICROBIOLOGICALLY INFLUENCED CORROSION

Brenda J. Little and Patricia A. Wagner
Naval Research Laboratory
Stennis Space Center, MS 39529

Zbigniew Lewandowski
College of Engineering, Montana State University
Bozeman, MT 59717

ABSTRACT

The relationship between biomineralization and microbiologically influenced corrosion (MIC) is intuitive—microorganisms influence corrosion by both forming and dissolving minerals. Biomineralization that results in mineral deposition on a metal surface can shift the corrosion potential in either a positive or negative direction, depending on the nature of the mineral. Manganese oxide biodeposition on stainless steel surfaces forces a shift in the positive, more noble direction, making some stainless steels more vulnerable to pitting and crevice corrosion. Bioprecipitated sulfides result in accelerated corrosion of some metals and alloys. Iron oxide formation can initiate a sequence of events that results in underdeposit corrosion of susceptible metals. Biomineral dissolution reactions remove passive layers or force mineral replacement reactions that lead to further dissolution. The role of biomineralization in MIC will be reviewed in the following sections.

Keywords: biomineralization, microbiologically influenced corrosion, oxides, sulfides

MINERAL DEPOSITION

Oxides

Biomineralization of iron and manganese oxides occurs widely in natural waters, and is a dominant control in geochemical cycling of these elements.[1] Mineralization can be carried out by a variety of organisms including bacteria, yeast, and fungi,[2] but is particularly associated with genera of the so-called iron and manganese bacteria, *Siderocapsa, Gallionella, Leptothrix, Sphaerotilus, Crenothrix,* and *Clonothrix.*

Manganese. Manganese oxidation is coupled to cell growth and metabolism of heterotrophic substrates.[3,4,5] While the reduced form of manganese generally identified as Mn^{2+} is soluble, all oxidized forms, Mn_2O_3, MnOOH,

Publication Right

Government work published by NACE International with permission of the author(s). Requests for permission to publish this manuscript in any form, in part or in whole must be made in writing to NACE International, Publications Division, P.O. Box 218340, Houston, Texas 77218-8340. The material presented and the views expressed in this paper are solely those of the author(s) and are not necessarily endorsed by the Association. Printed in the U.S.A.

Mn_3O_4, MnO_2, are insoluble. Microbially-deposited manganese oxides have an amorphous structure as vernadite (MnO_2) and sometimes form a black precipitate of birnessite (MnO_2) found with *Leptothrix* and spores of *Bacillus* spp.[1] In *Bacillus*, however, birnessite recrystallizes to octahedral hausmannite (Mn_3O_4).[2] The relationship of manganese-depositing bacteria with MnO_2 can be demonstrated with x-ray microscopy. In Figure 1 a *Pseudomonas*-like organism, originally isolated from freshwater,[4,5] is imbedded in the manganese oxides it produced. As a result of microbial action, manganese oxide deposits are formed on submerged materials including metal, stone, glass, and plastic and can occur in natural waters with manganese levels as low as 10–20 ppb.[6] Deposition rates of 1 mcoul cm^{-2} day^{-1} on stainless steel have been observed.[7] Mature manganese deposits from both fresh water and marine sources can be identified as ring structures that become more numerous and dense with time (Fig. 2a–d). Surfaces become covered with porous, blackened microbiologically-mediated manganese dioxide deposits (Fig. 2e).

Microbially-deposited manganese oxide on a stainless steel in fresh water (Fig. 3 a–c) caused an increase in E_{corr} and increased cathodic current density at potentials above –200 mV (vs saturated calomel reference electrode (SCE)).[7] For mild steel corrosion under anodic control, the oxides can elevate corrosion current but will cause little positive shift in E_{corr}. The increase in corrosion current may be significant for mild steel covered with biomineralized oxides and corrosion product tubercles that provide large mineral surface areas. Given sufficient conductivity in the tubercle (e.g. by magnetite), much of this material may serve as an oxide cathode to support corrosion at the oxygen-depleted anode within the tubercle. Continued biomineralization within the large tubercle may sustain a significant amount of the cathodic current. Both factors can increase the risk of stainless steel corrosion. Ennobled E_{corr} can reach pitting potentials for low molybdenum alloys, enhancing risk of pit nucleation, while elevated cathodic current density impedes repassivation. Biomineralized manganic oxides are efficient cathodes and increase cathodic current density on stainless steel by several decades at potentials between roughly –200 and +400 mV_{SCE}. The extent to which the elevated current density can be maintained is controlled by the electrical capacity of the mineral, reflecting both total accumulation and conductivity of the mineral-biopolymer assemblage (only material in electrical contact with the metal will be cathodically active). Oxide accumulation is controlled by the biomineralization rate and the corrosion current, in that high corrosion currents will discharge the oxide as rapidly as it is formed. This variation in accumulation causes the oxides to exert different modes of influence on the corrosion behavior of active metals compared with passive metals.

Iron. Iron-depositing bacteria produce orange-red tubercles of iron oxides and hydroxides by oxidizing ferrous ions from the bulk medium or the substratum (Fig. 4). Using environmental scanning electron microscopy (ESEM) it is possible to demonstrate iron-depositing bacteria within tubercles as twisted filaments with iron-rich deposits along their length (Fig. 5). Iron-depositing bacteria are microaerophilic and may require synergistic associations with other bacteria to maintain microaerophilic conditions in their immediate environment. Bacilli and cocci were imaged on the surface of the tubercle in Figure 4. Deposits of cells and metal ions create oxygen concentration cells (Fig. 6) that effectively exclude oxygen from the area immediately under the deposit and initiate a series of events that are individually or collectively very corrosive. In an oxygenated environment, the area immediately under individual deposits becomes deprived of oxygen. That area becomes a relatively small anode compared to the large surrounding oxygenated cathode. Cathodic reduction of oxygen may result in an increase in pH of the solution in the vicinity of the metal. The metal will form metal cations at anodic sites. If the metal hydroxide is the thermodynamically stable phase in the solution, the metal ions will be hydrolyzed by water with the formation of H^+ ions. If cathodic and anodic sites are separated from one another, the pH at the anode will decrease and that at the cathode will increase. In addition, Cl^- ions from the electrolyte will migrate to the anode to neutralize any buildup of charge, forming heavy metal chlorides that are extremely corrosive. Under these circumstances, pitting involves the conventional features of differential aeration, a large cathode to anode surface area and the development of acidity and metallic chlorides. Pit initiation depends on mineral deposition by bacteria. Pit propagation depends on alloying elements.[8] This means that attempts to kill the organisms within mineral deposits using biocides will not result in a cessation of pit propagation.[9] Stainless steels containing 6% or more molybdenum are not vulnerable to this type of attack.

Sulfides

Many sulfide minerals under near-surface natural environmental conditions can only be produced by microbiological action on specific precursor materials such as metals. Sulfate-reducing bacteria (SRB) are a diverse group of anaerobic

bacteria that can be isolated from a variety of environments[10,11] including seawater where the concentration of sulfate is typically 25 mM.[11] Even though seawater is generally aerobic (typical oxygen values above the thermocline are in the range 4–6 ppm), anaerobic microorganisms survive in anaerobic microniches until conditions are suitable for their growth.[12,13] If the aerobic respiration rate within a biofilm is greater than the oxygen diffusion rate, the metal/biofilm interface can become anaerobic and provide a niche for sulfide production by SRB.[14] Conversion of metals to sulfide minerals by SRB has been studied since the late 1800s.[15,16] Baas-Becking and Moore[17] list sulfides produced by *Desulfovibrio desulfuricans* over a large pH range.

In the following sections, SRB sulfide production will be reviewed for iron, copper, silver, zinc and lead. The metal interface under the biofilm and corrosion layers will be referred to as base metal to differentiate it from layers of minerals and metal ions that have been derivatized by corrosion reactions. Mineralogical data, thermodynamic stability diagrams[18,19] and the simplexity principle for precipitation reactions[20] will be used to rationalize corrosion product mineralogy in fresh and saline water and to demonstrate the action of SRB.

Iron. The corrosion rate of iron in the presence of hydrogen sulfide is accelerated by the formation of iron sulfide minerals.[21] Once electrical contact is established, mild steel behaves as an anode and electron transfer occurs through the iron sulfide. In the absence of oxygen, the metabolic activity of SRB causes accumulation of hydrogen sulfide near metal surfaces. This is particularly evident when metal surfaces are covered with biofilms. Figure 7 shows concentration profiles of sulfide, oxygen, and pH in a biofilm accumulated on the surface of a mild steel corrosion coupon. The concentration of sulfide is highest near the metal surface where iron sulfide forms quickly and covers the steel surface if both ferrous and sulfide ions are available. At low ferrous ion concentrations, adherent and temporarily protective films of iron sulfides are formed on the steel surface with a consequent reduction in corrosion rate. High rates of SRB-induced corrosion of mild steel are maintained only in high concentrations of ferrous ion.

Figure 8 is a stability diagram for an iron-water-reduced sulfur system with lines for 10^{-6} M ferrous iron and 10^{-2} M sulfide. For clarity, pyrite (FeS_2) and mackinawite (FeS_{1-x}) are the only sulfides indicated. Parallelograms superimposed on the diagram are bounded by the highest and lowest pH values commonly found in natural fresh and saline surface waters. The upper portion of the hatched area applies to waters less than 10 meters from the surface; the lower portion (oppositely hatched) represents waters at depths greater than 10 meters. Conditions in the upper hatched parallelogram represent those readily achieved in stagnant waters. The lower portion indicates conditions not found in near-surface environments. Mackinawite is a tetragonal mineral that may be unstable altogether but is clearly unstable above 150°C. It cannot be produced by conventional techniques. Greigite is a thiospinel with formula Fe_3S_4. Smythite is a hexagonal compound with formula $Fe_{3-x}S_4$, $0<x<0.25$. Cubic FeS can be produced artificially. By applying H_2S pressures in the range of one atmosphere, Berner[22] produced "tetragonal FeS" which has the same symmetry as mackinawite but contains somewhat less sulfur and has slight but systematic differences in lattice parameters. Presumably, further increases in H_2S pressure could produce material equivalent to natural mackinawite. Thermodynamic analyses indicate that, under redox and sulfide activity conditions in surface waters, only pyrite is stable; furthermore, pyrite forms relatively easily in nonbiological corrosion, so the preferential formation of less stable sulfides is difficult to attribute to slow pyrite formation kinetics. The region of stability for pyrite is accessible under severe conditions. The region of stability of mackinawite is wholly outside the region defined by surface water conditions, excluding waters influenced by peat bogs, coal mines, volcanic activity and industrial effluents.

During corrosion of iron and steel in the presence of SRB, a thin (approximately 1 μm), adherent layer of "tarnish" is first formed. This was originally termed "kansite," but has since been identified as mackinawite. As it thickens, the layer becomes less adherent. If ferrous ion concentration in the electrolyte is low, the mackinawite alters to greigite. This alteration is not observed in nonbiological systems. If ferrous ion concentration is high, mackinawite is accompanied by green rust 2, a complex ferrosoferric oxyhydroxide. The presence of green rust 2 may be due to a solubility effect and accounts for reduced corrosion rates when the electrolyte is rich in ferrous ions and has a very low renewal rate.

In summary, mackinawite is easily produced from iron and iron oxides by consortia of microorganisms that include SRB. The presence of mackinawite in corrosion products formed in shallow water environments with the

exclusions previously delineated is proof that the corrosion was SRB-induced. Recent work indicates that on continued exposure to SRB mackinawite alters to greigite (Fe_3S_4), smythite (Fe_9S_{11}) and finally to pyrrhotite (FeS_{1+x}).[23] SRB in thin biofilms on pottery surfaces[24,25] and silver[26] can produce pyrite films from iron-rich waters. Pyrite is not a typical iron corrosion product, but SRB can produce pyrite from mackinawite in contact with elemental sulfur.[22] Abiotic aqueous synthesis of these minerals, with the possible exception of pyrite, requires H_2S pressures higher than those found in shallow waters.

Copper. Cuprite (Cu_2O), the first product of copper corrosion, forms epitaxially as a direct reaction product of copper with dissolved oxygen or with water molecules.[27] Cuprite has a high electrical conductivity and permits transport of copper ions through the oxide layer so they can dissolve in the water and reprecipitate. If the water chemistry approximates that of seawater, copper ions reprecipitate as botallackite ($Cu_2(OH)_3Cl$)[28] which can alter in minutes or hours to either paratacamite or atacamite (other crystal structures of $Cu_2(OH)_3Cl$) depending on local water chemistry. Paratacamite, the more common form, gives the appearance of having precipitated from solution, but may be a pseudomorph after botallackite.[29]

The impact of sulfides on the corrosion of copper alloys has received considerable attention, including published reports documenting localized corrosion of copper alloys by SRB in estuarine environments[30,31] and a report of the failure of copper alloys in polluted seawater containing waterborne sulfides that stimulate pitting and stress corrosion cracking.[32] Copper alloys suffer accelerated corrosion attack in seawater containing 0.01 ppm sulfide after 1-day exposure.[33] A porous layer of cuprous sulfide with the general stoichiometry $Cu_{2-x}S$, $O<x<1$ forms in the presence of sulfide ions.[34] Copper ions migrate through the layer, react with more sulfide, and produce a thick, black scale (Fig. 9).

Figure 10 is a stability diagram for copper and its minerals drawn for 10^{-6} M total dissolved copper and 10^{-2} M total sulfide. Parallelograms superimposed on the diagram are similar to those described for Figure 8 and are appropriate for the analysis of corrosion mineralogy under non-hydrothermal conditions. McNeil et al.[20] used Figure 10 to interpret results from laboratory experiments. They exposed mixed cultures known to contain SRB to copper and copper/nickel alloys in a variety of natural and synthetic waters containing sulfates for 150 days. The pH values of the waters, measured after two weeks, were between 5.5 and 6.8. All copper-containing metals exposed to SRB in isolated cultures and in the natural augmented waters were covered with black sulfur-rich deposits (Fig. 11). The thickness and tenacity of the surface deposits varied among the metals and cultures. Corrosion products on commercially pure copper were consistently nonadherent. Corrosion products on copper alloys were more adherent and in some cases difficult to scrape from the surface. In all cases, bacteria were closely associated with sulfur-rich deposits (Fig. 12 a–b). Many bacteria were encrusted with deposits of copper sulfides (Fig. 13). Most scanning electron microscopy (SEM) micrographs of SRB on copper surfaces indicate a monolayer of cells overlaying a sulfide layer. Transmission electron microscopy has been used to demonstrate that bacteria are intimately associated with sulfide minerals and that on copper-containing surfaces the bacteria were found between alternate layers of corrosion products and attached to base metal.[35]

Biomineralogy of copper sulfides has been studied for over a century.[15,16,17,34,36,37,38,39] The complexity of the resulting observations reflects the complexity of the copper-sulfur system, especially in the presence of alloying elements or iron in the environment.[40,41] Both high- and low-temperature polytypes of chalcocite (Cu_2S), digenite (Cu_9S_5), djurleite ($Cu_{1.93}S$–$Cu_{1.97}S$), anilite (Cu_7S_4), spionkopite ($Cu_{39}S_{28}$), geerite (Cu_8S_5), and covellite (CuS, generally blue-remaining) have been reported. In long-term corrosion where waters contain significant iron, chalcopyrite ($CuFeS_2$) is common.[15,16,42] While chalcopyrite films can be formed abiotically in high sulfur concentrations,[43] chalcopyrite and most other copper sulfides are not generally found as products of abiotic corrosion.

Detailed kinetics of individual reactions are not fully understood, and the consequences for corrosion depend on many factors, including mineral morphology and variations of redox and pH with time.[42] Discussions of alteration kinetics are contained in a number of papers.[17,44–47] The general phenomenology can be understood by the following approach. Microbial consortia that include SRB produce anoxic, sulfide-rich environments in which the conversion of copper to copper sulfides is thermodynamically favored at a concentration of 10^{-2} M total sulfur (Fig. 10). Reactions appear to proceed as suggested by Ostwald's rule: the first sulfur-poor compounds are converted to sulfur-rich compounds. One would expect a layering effect with covellite on the outside and chalcocite next to

unreacted copper metal. This has not been studied, and would be very difficult to study on pure copper because of the porous and mechanically unstable corrosion products. In short-term experiments with excess of copper over available sulfur, chalcocite with little or no covellite is formed.[20] Covellite is produced if excess sulfide is available, either deliberately provided[17] or naturally available.[15,36]

The presence of dissolved iron leads to other complications. Not only has chalcopyrite been observed, but also digenite,[17,20,36,48] djurleite[20,49] and the hexagonal high-temperature polytype of chalcocite.[20] These observations can be interpreted in terms of the simplexity principle[50]: impurities tend to stabilize high-entropy, high-temperature polytypes. Digenite stability is promoted by iron.[45] It appears that nickel stabilizes djurleite on copper-nickel and the stabilization of djurleite has major practical consequences. McNeil et al.[20] observed that corrosion layers showing strong digenite lines were never observed on pure copper, but frequently on copper-nickel alloys. Furthermore, corrosion products containing digenite showed substantial adherence and mechanical stability, while the corrosion products on pure copper, composed of chalcocite with only traces of other minerals, were powdery and nonadherent.

It has been argued that if the copper sulfide layer were djurelite, the sulfide layer would be protective.[51] Even if such a sulfide film were technically passivating, the mechanical stability of the film is so poor that sulfide films are useless for corrosion protection. In the presence of turbulence, the loosely adherent sulfide film is removed, exposing a fresh copper surface to react with sulfide ions. For these reasons, turbulence-induced corrosion and sulfide attack of copper alloys cannot easily be decoupled. In the presence of oxygen, the possible corrosion reactions in a copper sulfide system are extremely complex because of the large number of stable copper sulfides,[40] their differing electrical conductivities, and catalytic effects. Transformations between sulfides or of sulfides to oxides result in changes in volume that weaken the attachment scale and oxide subscale, leading to spalling. Bared areas repassivate forming cuprous oxide.

If conditions at the surface of a copper alloy permit precipitation of nantokite (CuCl) under the cuprite layer, the alloy becomes vulnerable to bronze disease[52] or pitting corrosion[53] depending on mass transport conditions. A biofilm containing acid-producing bacteria could help produce the requisite conditions by increasing acidity in anodic areas and reducing copper ion transport from the surface, producing a higher local concentration.[26] While nantokite-based corrosion can also occur by nonbiological paths, the nonisometric morphology frequently observed on precipitated cuprite crystals suggests that microbiological poisoning of growth planes is a factor. The presence of alloying elements does not protect against the formation of nantokite and the consequent bronze disease corrosion.[54]

Silver. Laboratory data on sulfide and derivation of silver can be summarized as follows: (1) corrosion of silver by reduced sulfides, whether H_2S[55,56] or organic sulfides[55] produces acanthite (monoclinic Ag_2S), (2) CS_2 does not produce corrosion, (3) the corrosivity of organic sulfides appears to be controlled by transport mechanisms and thus by vapor pressures, and (4) the rate of sulfidation is strongly affected by NH_3 and iron dissolved in the silver.[57] Abiotic aqueous corrosion of silver in the presence of reduced sulfur species produces acanthite in bulk.[58,59] Argentite (body-centered cubic Ag_2S) is observed when objects made of impure silver (e.g., coins) are corroded in sediments over archaeological periods.[48,60] If Cl^- is present acanthite or argentite combined with cerargyrite (AgCl) is formed.

These observations support the hypothesis that formation of argentite is limited to precipitation of a silver-copper sulfide by reduced sulfide species. This theory is consistent with the observation that argentite corrosion products are sometimes accompanied by jalpaite ($Ag_{1.5}Cu_{.5}S$).[48] Argentite made of pure silver is unstable at room temperature, yet there are two reasons why argentite should precipitate during MIC of archaeological objects. Argentite is usually associated with jewelry and coinage containing several percent copper. Argentite, unlike acanthite, can accommodate nearly 30% copper in its lattice.[61] The phenomenon is parallel to the production of akageneite ($\beta FeOOH$) rather than goethite ($\alpha FeOOH$) in the corrosion of meteorites which is attributed to the ability of the akageneite lattice to accommodate significant Cl^-, whereas the goethite lattice can accommodate little or none.[62] Precipitation of a mineral from an impure environment favors a loose crystal structure capable of accommodating impurity atoms.[50]

Argentite formation occurs when an object made of silver-copper alloy is in a water-saturated deposit containing SRB in a biofilm capable of maintaining reducing conditions, and bacteria (perhaps ammonia producers) capable of solubilizing silver and copper atoms. A layer of sand or soil restricts the ability of the metal ions to escape, so that concentrations of copper and silver ions within the biofilm rise to levels which cause precipitation. The precipitation of argentite is favored for the reasons given above. Jalpaite forms in regions where the copper concentration is high. Argentite and jalpaite could, in principal, be stabilized by corrosion of pure silver in a copper-rich environment, but for practical purposes the presence of either argentite or jalpaite implies that the silver artifact originally contained significant copper.

Other metals. SRB-induced corrosion of zinc produces a zinc sulfide reported to be sphalerite (ZnS).[17] SRB on lead carbonates produces galena (PbS).[23] Galena has been found more recently as a lead corrosion product in SRB-induced corrosion of lead-tin alloys.[42]

MINERAL DISSOLUTION

Biofilm formation on copper alloys often results in selective dealloying. Zinc tends to be selectively removed from copper-zinc alloys, producing a spongy copper material[63] Dealloying of copper from tin bronzes has been reviewed by Geilmann.[64] Partitioning of alloying elements between remaining metal ions in the corrosion product and the electrolyte has received little attention.[65]

Dissimilatory iron and/or manganese reduction occurs in several microorganisms, including anaerobic and facultative aerobic bacteria. Inhibitor and competition experiments suggest that Mn(IV) and Fe(III) are efficient electron acceptors similar to nitrate in redox ability and are capable of out-competing electron acceptors of lower potential, such as sulfate or carbon dioxide.[66] Many of the recently described metal-reducing bacteria are capable of using a variety of electron acceptors, including nitrate and oxygen.[66] Myers and Nealson [66] suggested that iron and manganese-reducing microorganisms must be in direct contact with oxides to reduce them. This conclusion is based on the observation that Fe(III) and Mn(IV) are not reduced if microorganisms capable of the reduction are separated from the oxides by a semi-permeable membrane that allows exchange of soluble molecules but prevents contact between the organism and the oxide. These experiments demonstrated that metal reduction by *Shewanella putrefaciens* required cell/surface contact and the rate of reduction was directly related to surface area. ESEM and confocal laser scanning microscopy (CLSM) images of bacteria during both the iron and manganese reduction processes showed close contact of the cells with the oxides during the early stages of reduction. In later stages manganese oxides were coated with a layer of extracellular material that obscured the cells.[67]

Little et al.[67] used synthetic iron oxides (goethite, α–FeO·OH; hematite, Fe_2O_3; and ferrihydrite, $Fe(OH)_3$) as model compounds to simulate the mineralogy of surface films on carbon steel. There is general agreement that oxide films formed on iron in air at temperatures below 200°C are composed of magnetite and hematite. Szklarska-Smialowska[68] described the formation of hematite over a magnetite film. Ferric oxyhydroxides, including goethite and lepidocrocite (γ–FeO·OH), have also been identified in protective layers on carbon steel. Under anaerobic conditions goethite, hematite, and ferrihydrite were reduced by *S. putrefaciens* (Table 1). Rates of reduction, measured by atomic absorption spectroscopy of Fe(II) in solution as a function of time, for the three minerals indicate that after a 24 hr exposure to *S. putrefaciens*, initial reduction rates for goethite and ferrihydrite were approximately the same and were 5× faster than the reduction rate for hematite. After 22 days the integrated reduction rates for goethite and ferrihydrite were much faster than those measured at 24 hr. The hematite reduction rate actually slowed over the exposure period so that after 22 days the overall integrated rate was 50× slower than reduction rates for goethite and ferrihydrite.[3,69] Differences in reduction rates may be due to surface areas of individual oxides. Mineralogy and crystal structure must also play a role in microbial attachment and rate of biomineralization.

Current noise measurements of carbon steel exposed to pure cultures of *S. putrefaciens* in media with and without the combination of sodium chloride and thiosulfate were used to monitor corrosion (Fig. 14a–b). In both cases current noise showed active surface changes. Fluctuations in noise records of a corroding metal are usually interpreted as being due to the sudden rupture of a protective oxide film followed by immediate repassivation *S. putrefaciens* can reduce thiosulfate to produce sulfide. Obuekwe et al.[70] evaluated corrosion of mild steel under conditions of simultaneous formation of ferrous and sulfide ions. They reported extensive pitting when both processes

were active. When only sulfide was produced, initial corrosion rates increased but later declined due to formation of a protective FeS film. High amounts of soluble iron prevent formation of protective sulfide layers on ferrous metals. Little et al.[67] attempted to isolate the impacts of iron and thiosulfate reduction on corrosion of carbon steel by controlling the electron acceptors available in the electrolyte. In the initial experiment, thiosulfate was added to the medium, while in the second it was removed. Substantial electrochemical noise was measured in both cases and both electrodes were pitted.

ESEM examination of carbon steel electrodes revealed extensive bacterial colonization after 1300 hr (Fig. 15a). The electrode was macroscopically pitted, and the location of pits coincided with colonies of bacteria (Fig. 15b). EDS analysis of the electrode surface showed that, like goethite and ferrihydrite, the modified surface, while still iron rich, had a complex mixture of elements, including phosphorous, sulfur, and chlorine (Fig. 15c). Mineral replacement reactions were documented by x-ray crystallography. After exposure to *S. putrefaciens* in anaerobic media, surface oxides were converted to ferrous phosphate.

CONCLUSIONS

Microorganisms influence corrosion of metals by both forming and dissolving minerals. Iron and manganese oxide deposition by bacteria make some metals more vulnerable to pitting and crevice corrosion by forcing the corrosion potential to the pitting potential or by initiating a sequence of events that results in underdeposit corrosion. Biomineral dissolution reactions remove passive layers or force mineral replacement reactions that lead to further dissolution. Recently developed techniques including environmental scanning electron and x-ray microscopies make it possible to determine spatial relationships between microorganisms within biofilms and minerals as they are formed, dissolved, or replaced.

Microorganisms within biofilms are capable of maintaining environments at biofilm/surface interfaces that are radically different from the bulk in terms of pH, dissolved oxygen, and other organic and inorganic species. As a consequence, microorganisms within biofilms produce minerals and mineral replacement reactions that are not predicted by thermodynamic arguments based on the chemistry of the bulk medium. For that reason, minerals within corrosion products can often be used as fingerprints for microbiologically influenced corrosion. For example, even though the region of stability predicted for mackinawite using stability diagrams is wholly outside the region defined by surface water E_h/pH conditions, excluding waters influenced by peat bogs, coal mines, volcanic activity and industrial effluents, mackinawite is easily produced from iron and iron oxides in surface waters by consortia of microorganisms that include SRB. The presence of mackinawite in corrosion products formed in shallow water environments, with the exclusions previously delineated, is proof that corrosion was SRB-induced.

ACKNOWLEDGMENTS

NRL Contribution Number NRL/PP/7333--97-0034. Work was performed under NRL Program Element 0601153N, Office of Naval Research contract no. N0001497WX30031 and Cooperative Agreement EEC-8907039 between the National Science Foundation and Montana State University.

REFERENCES

1. A. M. Gounot, FEMS Microbiol. Rev. 14(1994): p. 339.

2. K. Nealson, B. Tebo, R. Rosson, "Occurrence and Mechanisms of Microbial Oxidation of Manganese." In: Advances in Applied Microbiology V. 33, A. Laskin (ed.), (San Diego, CA: Academic Press, 1988), p. 279.

3. R. G. Arnold, T. DiChristina, M. Hoffmann, Biotechnol. Bioeng. 32(1988): p. 1081.

4. W. K. Jung, R. Schweisfurth, Z. fur Allg. Mikrobiologie 16, 2(1976): p. 133.

5. W. K. Jung, R. Schweisfurth, Z. fur Allg. Mikrobiologie 16, 8(1976): p. 587.

6. W. H. Dickinson, F. Caccavo, Z. Lewandowski, Corros. Sci. 38(1996): p. 1407.

7. W. H. Dickinson, Z. Lewandowski, Biofouling 10(1996): p. 79.

8. R. P. George, "Studies on the Corrosion and Tuberculation of Carbon Steel in Fresh Water, National Symposium of Research Scholars on Metals and Materials Research, (Madras, India: Indian Institute of Metals, 1996), p. 118.

9. J. D. A. Miller, A. K. Tiller, "Microbial Corrosion of Buried and Immersed Metal." In: Microbial Aspects of Metallurgy , J. D. A. Miller (ed.), (NY, NY: American Elsevier, 1970), p. 61.

10. N. Pfennig, F. Widdel, H. G. Truper, "The Dissimulatory Sulfate-Reducing Bacteria." In: The Prokaryotes: A Handbook on Habitats, M. P. Starr, et al., (eds.), (NY: Springer-Verlag, 1981), p. 926.

11. J. R. Postgate, The Sulphate-Reducing Bacteria. (Cambridge, UK: Cambridge University Press, 1979).

12. J. W. Costerton, G. G. Geesey, "The Microbial Ecology of Surface Colonization and of Consequent Corrosion." In: Biologically Induced Corrosion, S. C. Dexter (ed.), (Houston, TX: NACE International, 1986), p. 223.

13. E. E. Staffeldt, D. A. Kohler, Petrolia e Ambiente (1973): p. 163.

14. B. J. Little, P. A. Wagner, W. G. Characklis, W. Lee, "Microbial Corrosion," In: Biofilms, W. G. Characklis, K. C. Marshall (eds.), (NY, NY: John Wiley and Sons, 1990), p. 635.

15. G. A. Daubree, Bull. Soc. Geol. (France), 19(1862): p. 529.

16. M. de Gouvernain, Compt. Rend. 80(1875): p. 1297.

17. G. M. Baas-Becking, D. Moore, Econ. Geol. 56(1961): p. 259.

18. M. Pourbaix, Atlas of Electrochemical Equilibria in Aqueous Solutions, (Houston, TX: NACE International, 1966).

19. D. D. Wagman, W. H. Evans, V. B. Parker, R. H. Schumm, I. Halow, S. M. Bailey, K. L. Churney, R. L. Nuttall, NBS tables of chemical thermodynamic properties: selected values for inorganic and C_1 and C_2 organic substances in SI units. J. Phys. Chem. Ref. Data 11, supplement 2, 1982.

20. M. B. McNeil, J. Jones, B. J. Little, "Mineralogical Fingerprints for Corrosion Processes Induced by Sulfate-Reducing Bacteria," CORROSION/91, paper no. 580 (Houston, TX: NACE International, 1991).

21. A. G. Wikjord, T. E. Rummery, F. E. Doern, D. G. Owen, Corros. Sci. 20(1980): p. 651.

22. R. A. Berner, Econ. Geol. 64(1969): p. 383.

23. M. B. McNeil, B. J. Little, Corros. 46, 7(1990): p. 599.

24. S. J. Duncan, H. Ganiaris, "Some Sulphide Corrosion Products on Copper Alloys and Lead Alloys from London Waterfront Sites," In: Recent Advances in the Conservation and Analysis of Artifacts, E. J. Black (ed.), (Univ. London: Summer Schools Press, 1987), p. 109.

25. R. B. Heimann, Archeomaterials 31(1989): p. 123.

26. M. B. McNeil, D. W. Mohr, "Interpretation of Bronze Disease and Related Copper Corrosion Mechanisms in Terms of Log Activity Diagrams." In: Materials Problems in Art and Archaeology II, (Pittsburgh, PA: Materials Research Society, 1992), p. 1055.

27. R. F. North, M. J. Pryor, Corros. Sci. 10(1970): p. 297.

28. A. M. Pollard, R. G. Thomas, P. A. Williams, Mineralog. Mag. 53(1989): p. 557.

29. C. Kato, H. W. Pickering, J. Electrochem. Soc. 131(1984): p. 1219.

30. B. Little, P. Wagner, J. Jacobus, Mat. Perf. 27, 8(1988): p. 57.

31. B. Little, P. Wagner, J. Jacobus, L. Janus, Estuaries 12, 3(1989): p. 138.

32. J. C. Rowlands, J. Appl. Chem. 15(1965): p. 57.

33. J. P. Gudas, H. P. Hack, Corros. 35(1979): p. 67.

34. B. C. Syrett, "The Mechanism of Accelerated Corrosion of Copper-Nickel Alloys in Sulfide Polluted Seawater," CORROSION/80, paper no. 33, (Houston, TX: NACE International, 1980).

35. G. Blunn, "Biological Fouling of Copper and Copper Alloys." In: Biodeterioration VI, (Slough, UK: CAB Int., 1986) p. 567.

36. E. D. Mor, A. M. Beccaria, Br. Corros. J. 10(1975): p. 33.

37. B. C. Syrett, Corros. 33(1977): p. 257.

38. B. C. Syrett, Corros. Sci. 21(1981): p. 187.

39. M. B. McNeil, B. J. Little, J. Amer. Inst. for Conserv. 31, 3(1992): p. 355.

40. P. H. Ribbe (ed.), Sulfide Mineralogy, (Washington, DC: Mineralogical Society of America, 1976).

41. I. Kostov, J. Minceva-Stefanova, Sulphide Minerals, (Sofia, Bulgaria: Publishing House of the Bulgarian Academy of Sciences, 1981).

42. M. B. McNeil, D. W. Mohr, Geoarchaeol. 8, 1(1993): p. 23.

43. M. Cuthbert, Econ. Geol. 57(1962): p. 38.

44. E. H. Roseboom, Econ. Geol. 61(1966): p. 641.

45. J. R. Craig, S. D. Scott, "Sulfide Phase Equilibria," In: Sulfide Mineralogy, P. H. Ribbe (ed.), (Wash. DC: Mineralogical Society of America, 1976).

46. A. Putnis, Am. Mineralog. 62(1977): p. 107.

47. H. T. Evans, Z. Krist. 150(1979): p. 299.

48. N. North, I. D. MacLeod, "Corrosion of Metals." In: Conservation of Archaeological Objects, C. Pearson (ed.), (London: Butterworths, 1986) p. 69.

49. D. D. Macdonald, B. C. Syrett, S. S. Wing, Corros. 35(1979): p. 367.

50. J. Goldschmidt, J. Geol. 61(1953): p. 539.

51. I. Nilsson, S. Ohlson, L. Haggstrom, N. Molin, K. Mosbach, Europ. J. Appl Microbiol. Biotechnol. 10(1980): p. 261.

52. D. A. Scott, J. Amer. Inst. Conserv. 29(1990): p. 192.

53. V. F. Lucey, Br. Corros. J. 2(1967): p. 175.

54. L. Mond, G. Cuboni, Atti reale Accad dei Lincei serie 52(1893): p. 498.

55. J. D. Sinclair, Electrochem. Soc. 129(1982): p. 33.

56. L. Volpe, P. J. Peterson, Corros. Sci. 29(1989): p. 1179.

57. T. Biestek, M. Drys, Powlocki Ochronne (Warsaw) 9(1987): p. 2.

58. V. I. Birss, G. A. Wright, Electrochim. Acta 27(1981): p. 1.

59. G. D. Campbell, F. J. Lincoln, G. P. Power, I. M. Ritchie, Aust. J. Chem. 35(1982): p. 1079.

60. R. J. Gettens, "The Corrosion Products of Metal Antiquities," Annual Report to the Trustees of the Smithsonian Institution for 1963, The Freer Chinese Bronzes. Smithsonian Institution, Washington, 1963, p. 547.

61. V. V. Shcherbina, Geokhimiya 10(1978): p. 1444.

62. V. F. Buchwald, "The Mineralogy of Iron Meteorites," Phil. Trans. Roy. Soc., A286 (London, 1977): p. 453.

63. G. D. Walker, Corros. 33(1977): p. 252.

64. W. Geilmann, Angewandte Chemie 68(1956): p. 201.

65. E. I. Zolotarev, A. P. Pchel'mikov, YaB. Skuratnick, M. A. Dembrovskii, N. I. Khokhlov, V. V. Losev, Zashchita Metallov 23(1987): p. 922.

66. C. Myers, K. H. Nealson, Science 240(1988): p. 1319.

67. B. Little, P. Wagner, K. Hart, R. Ray, D. Lavoie, K. Nealson, C. Aguilar, "The Role of Metal-Reducing Bacteria in Microbiologically Influenced Corrosion," CORROSION/97, paper no. 215, (Houston, TX: NACE International, 1997).

68. Z. Szklarska-Smialowska, Pitting Corrosion of Metals, (Houston, TX: NACE International, 1986).

69. E. E. Roden, J. M. Zachara, Environ. Sci. & Tech. 30(1996): p. 1618.

70. C. O. Obuekwe, D. W. S. Westlake, J. A. Plambeck, F. D. Cook, Corros. 37, 8(1981): p. 461.

TABLE 1
RELATIVE RATES OF IRON REDUCTION BASED ON Fe(II) IN SOLUTION

	24 Hours mg/L/d	% Max	22 Days mg/L/d	% Max
Goethite	3.50	100	18.20	100
Ferrihydrite	2.60	74	14.10	77
Hematite	0.58	22	0.39	2

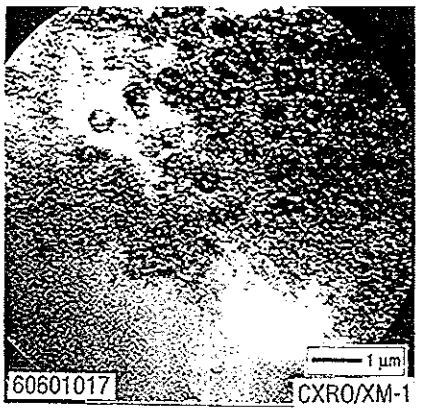

FIGURE 1 — X-ray micrograph of manganese-depositing bacterial cells with manganese oxides. Cells are dark ellipses, oxides are lighter material. (Unpublished micrograph produced at the Center for X-ray Optics, Lawrence Berkeley Laboratories, Berkeley, CA, produced by B. Tonner, W. Meyer-Ilse and J. Brown from samples provided by K. Nealson, University of Wisconsin, Milwaukee, WI).

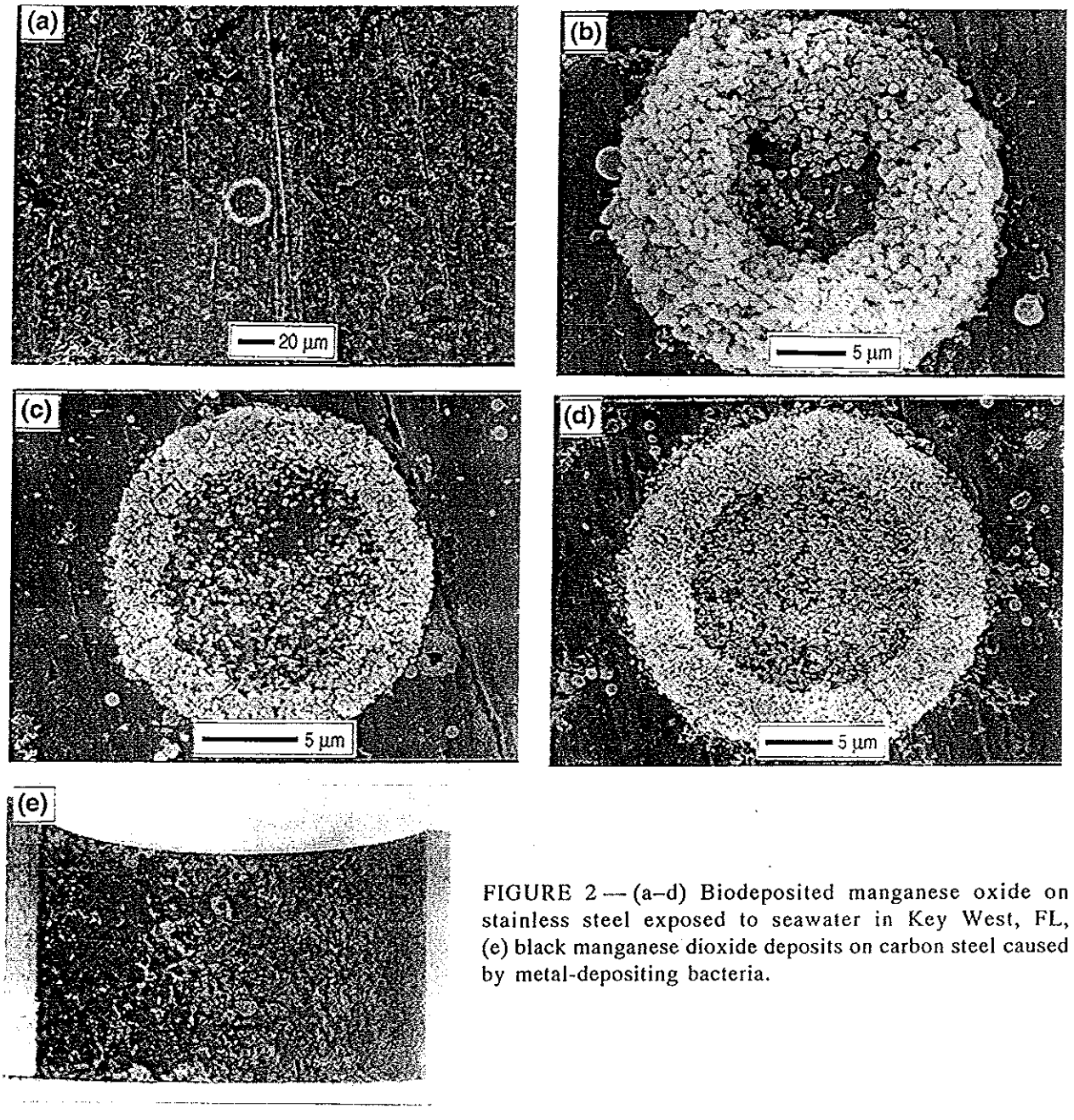

FIGURE 2 — (a–d) Biodeposited manganese oxide on stainless steel exposed to seawater in Key West, FL, (e) black manganese dioxide deposits on carbon steel caused by metal-depositing bacteria.

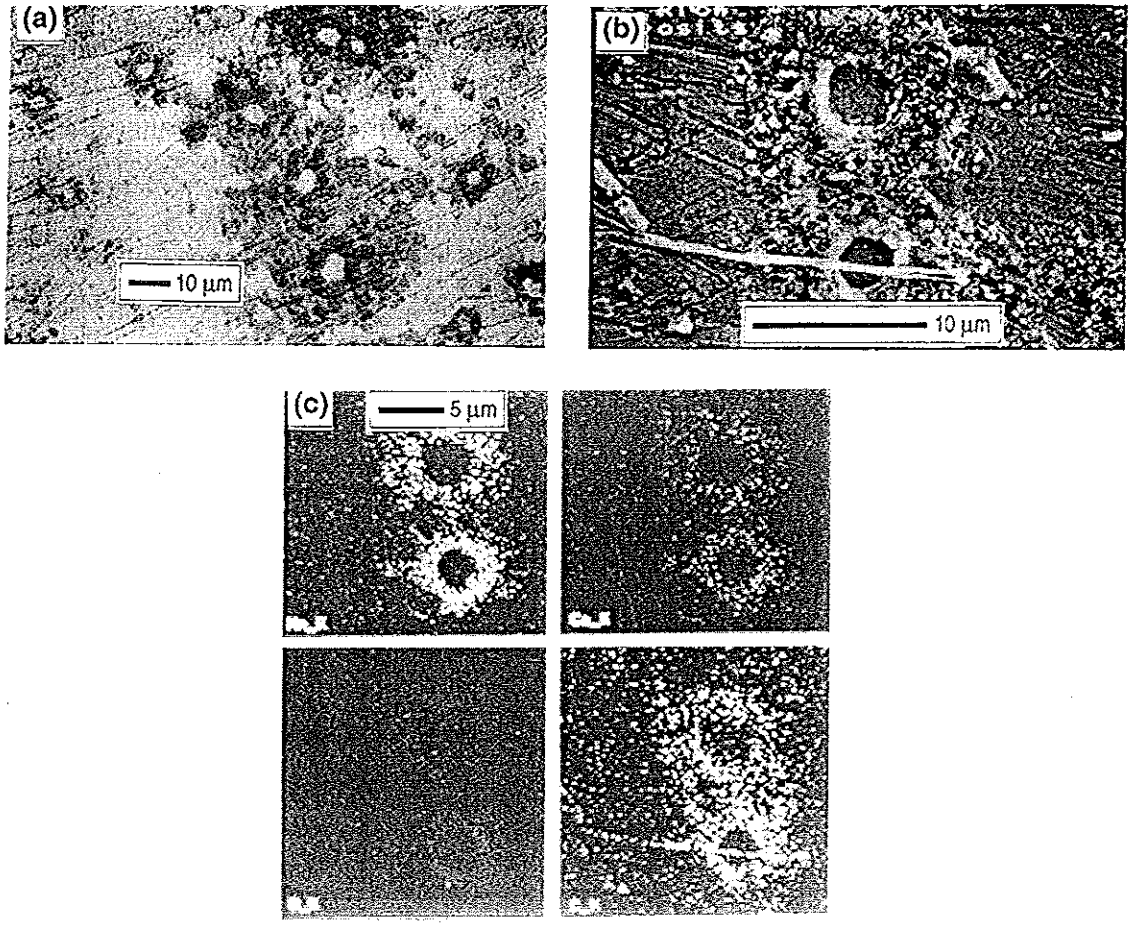

FIGURE 3 — Annular deposits on stainless steel after 13 days exposure to fresh water, (a) reflected light micrograph,[7] (b) SEM micrograph,[6] and (c) energy dispersive spectroscopy (EDS) maps of two adjacent annular deposits confirming the presence of manganese, calcium, oxygen, and carbon in the deposits [6] ("Reprinted from Ref. 6 with kind permission from Elsevier Science Ltd, The Boulevard, Langford Lane, Kidlington 0X5 1GB, UK".).

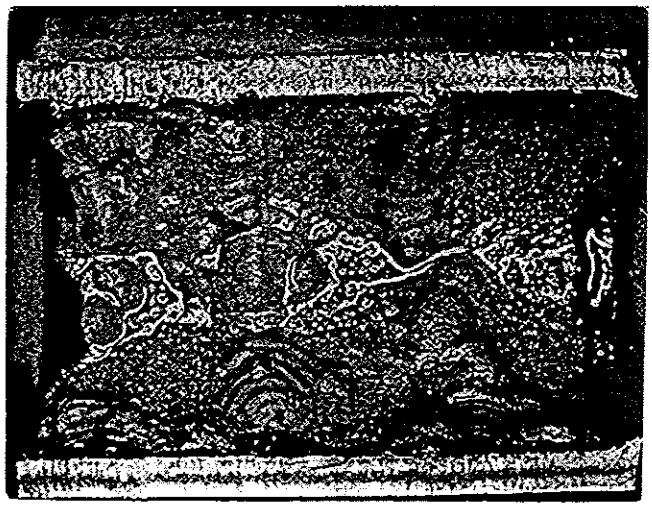

FIGURE 4 — Iron oxide deposits on galvanized pipe (2×).

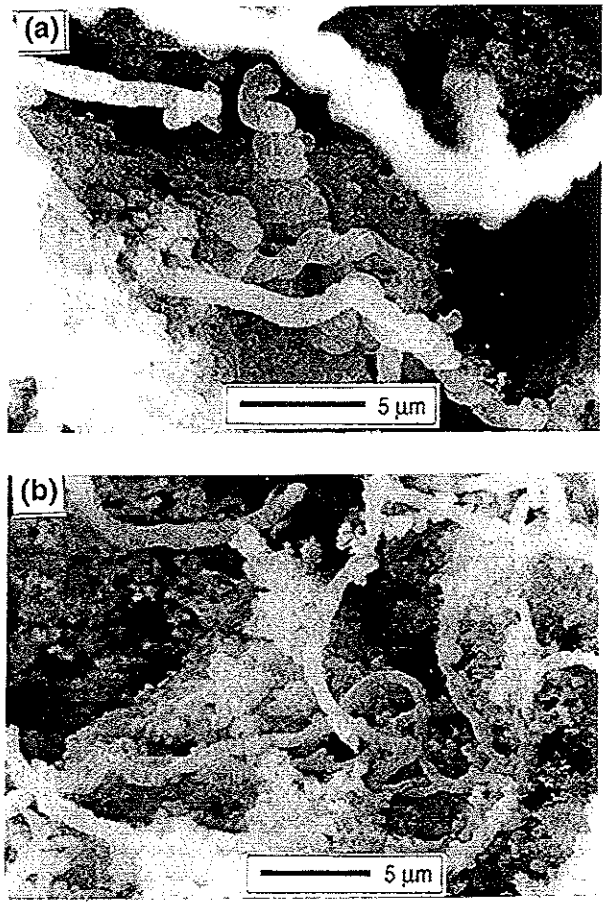

FIGURE 5 — ESEM micrograph showing iron-depositing bacteria within tubercles from Figure 4.

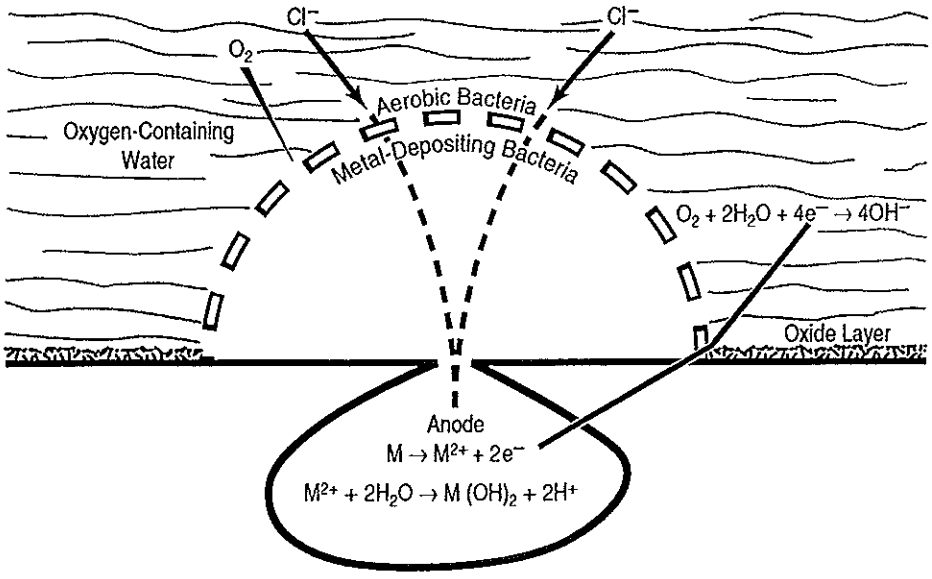

FIGURE 6 — Possible reactions under tubercles created by metal-depositing bacteria.

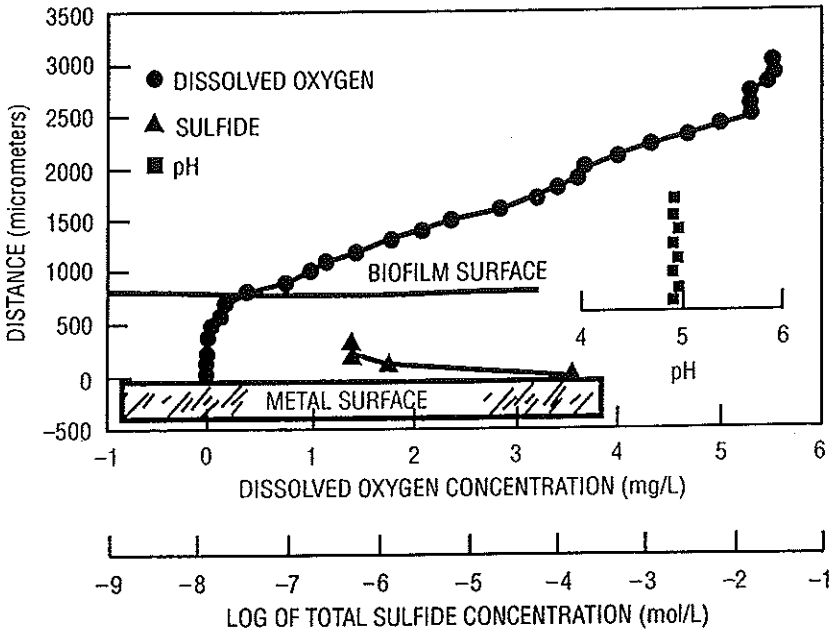

FIGURE 7 — Concentration profiles of sulfide, oxygen, and pH in a biofilm on mild steel. (Reprinted with permission from W. Lee, Z. Lewandowski, M. Morrison, W. G. Characklis, R. Avsi, P. Nielsen, Biofouling 7(1993): p. 217).

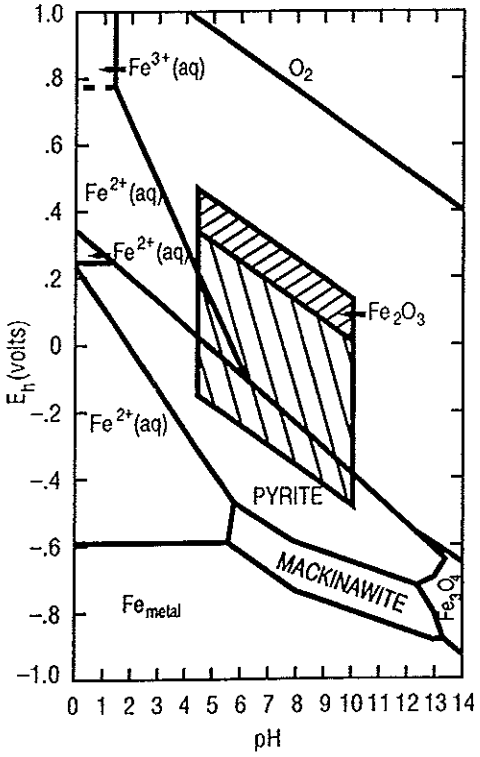

FIGURE 8 — Iron stability diagram: water without chloride irons, total sulfide 10^{-2} M.

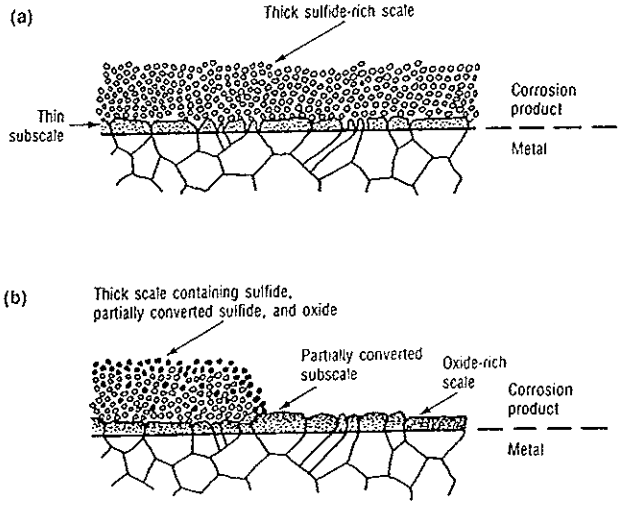

FIGURE 9 — Schematic of (a) thick sulfide-rich scale on copper alloy and (b) disruption of sulfide film.[38]

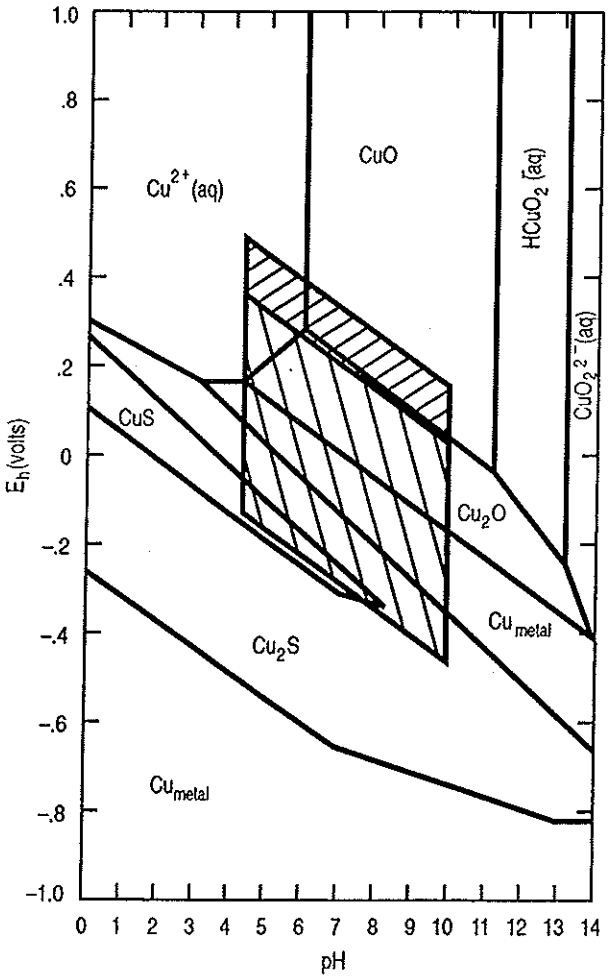

FIGURE 10 — Copper stability diagram: water without chloride ions, total sulfide 10^{-2} M.



FIGURE 11 — Black sulfide film on copper foil after 4-month exposure to SRB.

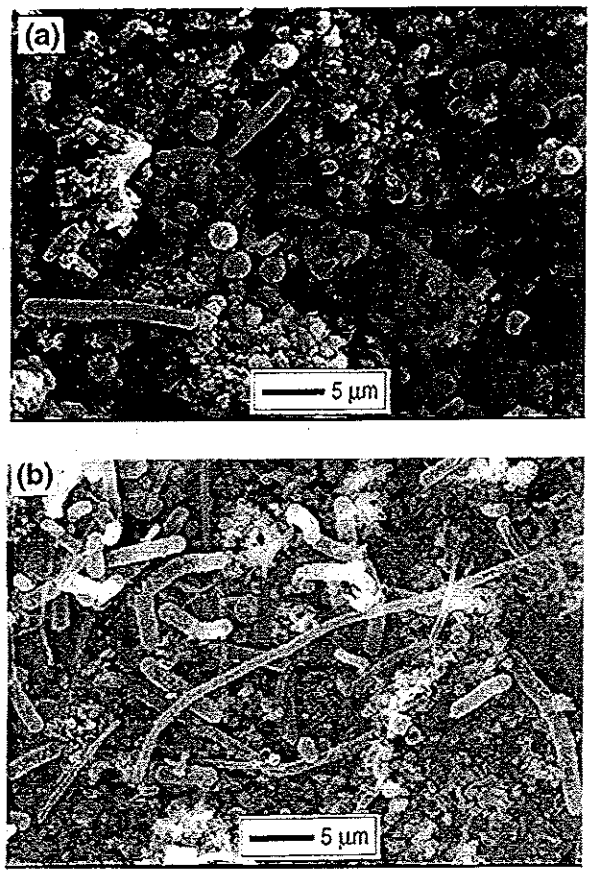

FIGURE 12 — (a,b) ESEM micrographs of bacteria within corrosion products on copper-containing foils.

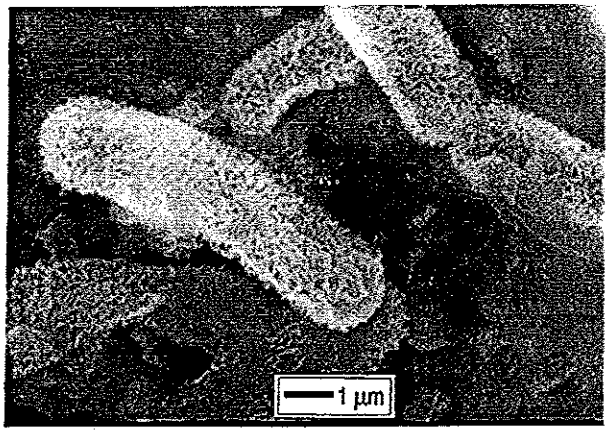

Figure 13. ESEM micrograph showing encrustations of copper sulfide on bacterial cells.

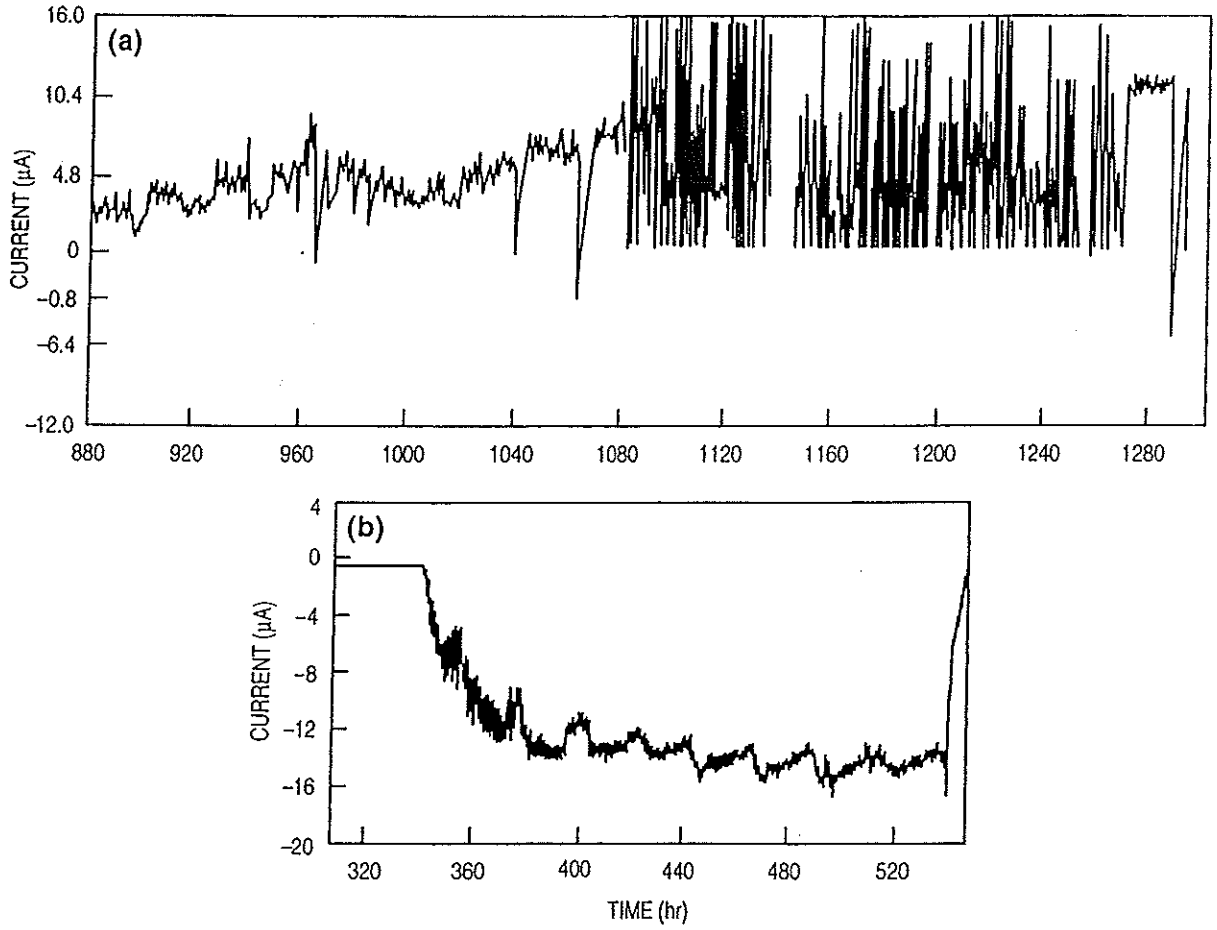

Figure 14. Electrochemical noise plots for carbon steel exposed to *S. putrefaciens*: (a) in medium containing thiosulfate and sodium chloride and (b) in medium without thiosulfate and sodium chloride.

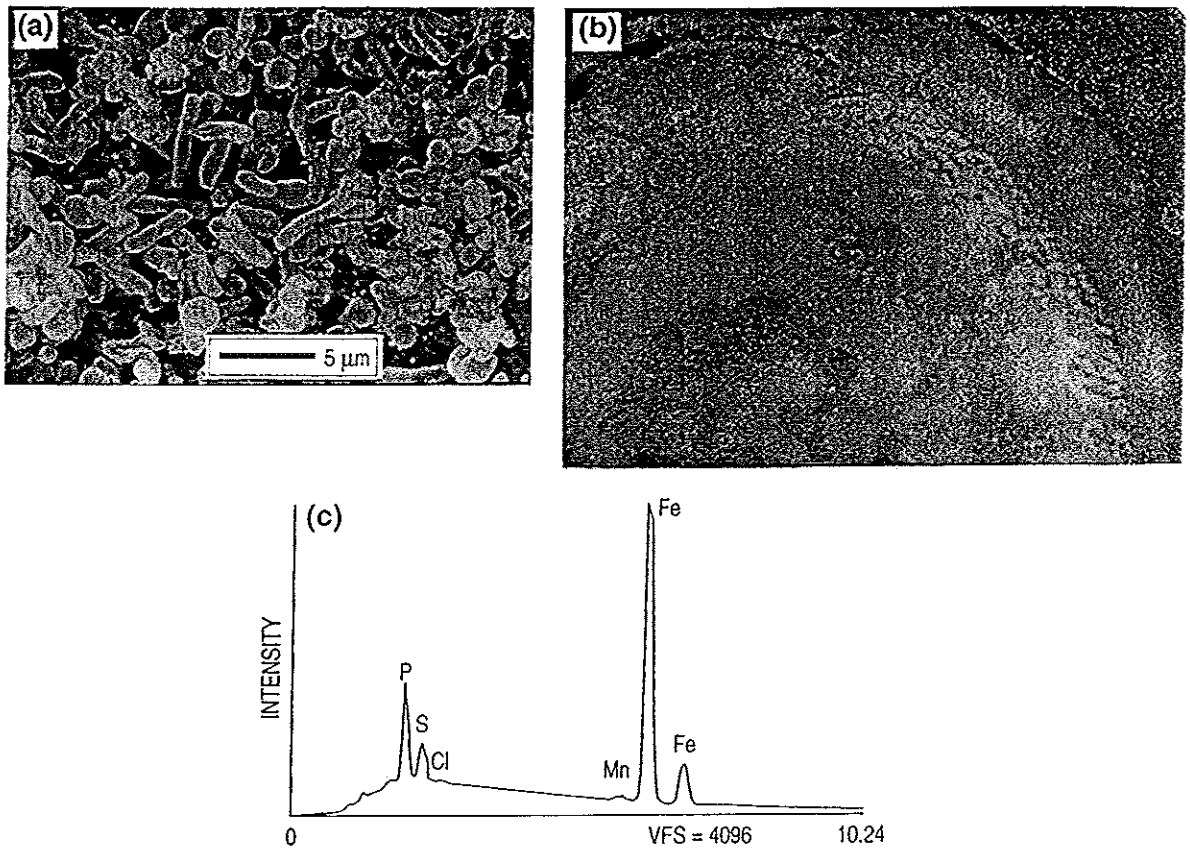

FIGURE 15 — ESEM micrographs of carbon steel electrode after 1300 hr exposure to *S. putrefaciens* (a) bacterial colonization, (b) surface pitting (12×), and (c) EDS of surface.